Novel Scheelite-Type $[Ca_{0.55}(Nd_{1-x}Bi_x)_{0.3}]MoO_4$ ($0.2 \leq x \leq 0.95$) Microwave Dielectric Ceramics with Low Sintering Temperature

Shu-Zhao Hao,[a] Di Zhou,[a*] Fayaz Hussain,[b] Jin-Zhan Su,[c] Wen-Feng Liu,[d] Da-Wei Wang,[e] Qiu-Ping Wang[f] and Ze-Ming Qi[g]

[a]Electronic Materials Research Laboratory, Key Laboratory of the Ministry of Education & International Center for Dielectric Research, School of Electronic and Information Engineering, Xi'an Jiaotong University, Xi'an 710049, China

[b]Department of Materials Engineering, NED University of Engineering & Technology, Karachi, 75270, Pakistan

[c]International Research Centre for Renewable Energy, State Key Laboratory of Multiphase Flow in Power Engineering, Xi'an Jiaotong University, Xi'an, Shaanxi 710049, China

[d]State Key Laboratory of Electrical Insulation and Power Equipment, Xi'an Jiaotong University, Xi'an 710049, Shaanxi, China

[e]Department of Materials Science and Engineering, University of Sheffield, Sheffield S1 3JD, United Kingdom

[f]School of Science, Xi'an Polytechnic University, Xi'an 710048, China

[g]National Synchrotron Radiation Laboratory, University of Science and Technology of China, Hefei, Anhui 230029, China

*Corresponding author E-mail address: zhoudi1220@gmail.com (Di Zhou)

This article has been accepted for publication and undergone full peer review but has not been through the copyediting, typesetting, pagination and proofreading process, which may lead to differences between this version and the Version of Record. Please cite this article as doi: 10.1111/JACE.17378

Abstract

Novel scheelite-type $[Ca_{0.55}(Nd_{1-x}Bi_x)_{0.3}]MoO_4$ ($0.2 \leq x \leq 0.95$) ceramics were prepared using the solid-state reaction method. According to the X-ray diffraction data, a solid solution was formed in $0.2 \leq x \leq 0.95$ and all the samples belong to pure scheelite phase with the tetragonal structure. As revealed by Raman spectroscopy, the number of vibrational modes decreased with the increase of x value, which further indicated that Bi^{3+} ions occupied A-site of scheelite structure. As the x value increased, the sintering temperature decreased from 740 ℃ to 660 ℃; the permittivity increased from 12.6 to 20.3; the Qf value first decreased slightly and gradually remained stable. Based on the infrared reflectivity spectrum analysis, the calculated permittivity derived from the fitted data shared the same trend with the measured value. The $[Ca_{0.55}(Nd_{0.05}Bi_{0.95})_{0.3}]MoO_4$ ceramic sintered at 660 ℃ attained a near-zero value temperature coefficient ~ τ_f (-7.1 ppm/℃) and showed excellent microwave dielectric properties with a ε_r ~ 20.3 and a Qf ~ 33,860 GHz, making this system a promising candidate in the ultra-low temperature co-fired ceramic (ULTCC) technology.

Keywords: LTCC; Raman spectra; infrared spectra; low-sintering

1. INTRODUCTION

Microwave device is an important part of the modern wireless communication system, with the 5th generation wireless systems coming. The investigation of microwave ceramic is drawing more and more attention.[1] Meanwhile, a series of new materials manufacturing process, such as the low-temperature co-fired ceramic (LTCC) technology and the ultra-low temperature co-fired ceramic (ULTCC) technology,[2] provide technical support for the fabrications of the miniaturized and integrated microwave devices. Hence, there is an urgent need to develop microwave ceramics suitable for LTCC/ULTCC technology. Microwave dielectric ceramics used in LTCC/ULTCC technology must meet several basic requirements. First, the microwave ceramics should have lower sintering temperatures than the melting points (MP) of metal electrodes, such as Ag with a MP ~ 961 ℃ and Al with a MP ~660 ℃. Second, the dielectric loss should be very low (high quality factor Q) to reduce the power consumption of microwave devices. Third, the temperature coefficient of resonant frequency τ_f values of the microwave ceramics should approach the zero to improve the temperature independence of microwave devices. Finally, the raw materials of the microwave ceramics should be nontoxic for the environment.[3-10]

Recently, the $A^{2+}B^{6+}O_4$ (A^{2+} = Mg, Mn, Ca, Zn, Cd, and B^{6+} = Mo, W) oxides with scheelite structure have been widely investigated on their microwave dielectric properties.[11,12] Due to the low sintering temperature and the adaptive crystal structure providing the potential for the various substitutions at A- or B-site, these compositions have received extensive attentions in LTCC technology. In the previous report, Choi et al. found that the $CaMoO_4$ possessed a high Qf value (~89,700 GHz) and a low sintering temperature (~1100 ℃).[13] Rama *et al*. used the Cd^{2+} ion to substitute for the Ca^{2+} ion and gained good microwave dielectric properties (ε_r = 8 ~ 10, Qf = 46,000 ~ 53,000 GHz, τ_f = -22 ~ -57 ppm/ ℃) in $Ca_{1-x}Cd_xMoO_4$ ceramics at low temperature (900 ~ 1075 ℃).[14] Zhou *et al*. changed the elements at A-site and gained the temperature stable $[(Li_{0.5}Ln_{0.5})_{0.2}Ca_{0.8}]MoO_4$ ceramics with excellent microwave dielectric properties (ε_r = 10.6 ~ 11, Qf =18,400 ~ 24,500 GHz, τ_f = -7.1~ + 6.9 ppm/℃) and low sintering temperatures (S.T = 800 ~ 900 ℃).[15,16] According to the literatures' reports,[17,18] the $CaMoO_4$ ceramic has a negative τ_f value, and the Bi-doping could adjust the τ_f to near-zero and even positive value. The bismuth oxide was reported to have intrinsic low melting temperature and might help reduce the sintering temperature of scheelite oxides. Besides, the rare earth oxide, such as Nd_2O_3 etc., was found to improve the dielectric property in many microwave dielectric ceramics.[19] The microwave dielectric properties are closely related to the microstructures of ceramics. Choi *et al*. ever used the Clausius–Mosotti relation to calculate the polarizability of Mo in $AMoO_4$ (A = Mg, Zn, Sr, Ca and Ba) compounds.[13] Kim *et al*. used the packing fraction to correlate the quality factor of scheelite $A^{2+}B^{6+}O_4$ oxides.[20] Furthermore, many researchers used the Raman spectroscopy to obtain the information of the vibrations and rotations.[21,22] Some researchers used the infrared spectroscopy to reveal the complex dielectric response in ceramics.[23,24] Based on the fitting data from the infrared spectroscopy, the permittivity and intrinsic dielectric losses could be calculated. Hence, in this work, the $(Nd_{1-x}Bi_x)^{3+}$ complex ions were used at A-site of scheelite

structure to adjust the microwave dielectric properties and the sintering temperature of $CaMoO_4$ ceramic. The micro-characteristics and microwave dielectric properties of $[Ca_{0.55}(Nd_{1-x}Bi_x)_{0.3}]MoO_4$ ($0.2 \leq x \leq 0.95$) ceramics were studied. The relationship between the properties and vibrational modes were investigated in detail.

2. EXPERIMENTAL SECTION

High-purity oxide powders of Bi_2O_3 (>99%), MoO_3 (>99.95%), Nd_2O_3(>99%) and the carbonate powder of $CaCO_3$ (>99%) were mixed proportionally for the $[Ca_{0.55}(Nd_{1-x}Bi_x)_{0.3}]MoO_4$ ($0.2 \leq x \leq 0.95$) ceramics. First, the raw materials were put into the nylon jars with zirconia balls and prepared by the method of high energy milling. Second, the milled powders were calcined at 600 ℃ for 4 h. Then, the calcined powders were ground for the second time. After the milled powders were dried, the PVA binder can be used to mix the powders and make the powders granulated. Finally, the mixed powders were pressed into pillars under a pressure of 160 MPa by using the uniaxial hydraulic press. All the green bodies were put into the muffle and sintered at the temperature from 660 ℃ to 740 ℃, the holding time is 2 h.

Phase identifications of the samples were obtained by the powder diffraction data using the X-ray diffractometer with Cu Kα source, operated at 40kV and 30mA, all the data were gathered in the range of 10-70° with a scan step of 0.02. The topography of the crystal grain of the ceramics was surveyed using the scanning electron microscopy (SEM). The IR spectra measurement of the ceramics used a Bruker Optik IFS 66v FTIR spectrometer on an infrared source base station (U4) at the National Synchrotron Radiation Lab. (NSRL), China. The measurement of the Raman vibration modes of the ceramics used a Raman spectrometer, which was stimulated using an Ar^+ laser (532 nm). The quality factor was measured with a microwave network analyzer and the dielectric constant was calculated with the $TE_{01\delta}$ shielded cavity method, meanwhile, the τ_f value was measured in a thermal cycling chamber, the calculated value could be obtained using the the following formula:

$$\tau_f = \frac{f_h - f_l}{f_l(h-l)} ppm/°C \quad (1)$$

where the h and l were the values of high temperature and low temperature, respectively. The f_h was the $TE_{01\delta}$ resonant frequencies at high temperature, and the f_l was the $TE_{01\delta}$ resonant frequencies at low temperature.

3. RESULTS AND DISCUSSIONS

In Fig.1 (a), the room temperature XRD patterns and the crystal structure (Inset) of the $[Ca_{0.55}(Nd_{1-x}Bi_x)_{0.3}]MoO_4$ ceramics are clearly observed. All the diffraction peaks are indexed as a tetragonal scheelite structure without any secondary phase.[25] Therefore, the complete solid solution is obtained in the whole compositions. With the increase of x value, the corresponding peaks moved to lower 2θ angles direction, which indicates an increase of the unit cell volume. According to the ionic radius reported by Shannon,[26] the ionic radius of Bi^{3+} (1.17Å) is larger than that of Nd^{3+} (1.109Å) and introduction of Bi^{3+} expanded the volume of the unit cell. Meanwhile, the intensity of (101) peak gradually decreases, indicating that the increase of content

of Bi^{3+} ions enhanced the disordering at A-site.[27] The lattice parameters calculated from the measured XRD data are shown in Fig.1 (b). When the *x* value increases, the lattice parameters *a*, *c* and the unit cell volume *V* all increase, which are consistent with the peaks shifts in XRD patterns. Meanwhile, a slight decrease in *a*/*c* could be observed as shown in Fig.1(b).

SEM images of the $[Ca_{0.55}(Nd_{0.8}Bi_{0.2})_{0.3}]MoO_4$ ceramic sintered at 740 ℃ is shown in Fig.2 (a). The sample has dense microstructure and no pores could be revealed in this composition. The grain size distribution of the $[Ca_{0.55}(Nd_{0.8}Bi_{0.2})_{0.3}]MoO_4$ ceramic is presented in inset of Fig.2 (a), the average grain size is about 3.16 μm. As shown in Fig.2 (b), the homogeneous microstructure of $[Ca_{0.55}(Nd_{0.05}Bi_{0.95})_{0.3}]MoO_4$ ceramic sintered at 660 ℃ can be observed. As shown in inset of Fig.2 (b), the mean grain size is about 2.78 μm, which is smaller than the grain size of $[Ca_{0.55}(Nd_{0.8}Bi_{0.2})_{0.3}]MoO_4$ ceramic. This result indicates that the increasing concentration of Bi^{3+} ion reduced both the sintering temperature and grains size.

Raman spectrum is a very important tool to investigate the influence of the ionic substitution at A-site in inorganic compounds. The $[Ca_{0.55}(Nd_{1-x}Bi_x)_{0.3}]MoO_4$ ceramics belong to the tetragonal scheelite structure with $I4_{1/a}$ space group. According to the group theory, there may be 26 modes in the components, the calculated results show as follows:

$$\Gamma = 3A_g + 5B_g + 5E_g + 5A_u + 5E_u + 3B_u \quad (2)$$

In the scheelite primitive cell, the A_g, B_g and E_g vibrations are Raman active vibrations, the A_u and E_u belong to the infrared active vibrations and the B_u is the inactive vibrations. Furthermore, as the literature reported,[28] the lattice vibrations are divided into two parts in the tetragonal scheelite structured materials. The first one is external mode, which correspond to the movements of A-site cations and rigid Mo-O tetrahedra, the measured data below 350 cm^{-1} all belong to the external modes. The second one is internal mode, which derive from the vibrations inside the Mo-O tetrahedra, the measured data above 350 cm^{-1} all belong to the internal modes.

In the present study, Raman spectra of $[Ca_{0.55}(Nd_{1-x}Bi_x)_{0.3}]MoO_4$ ceramics are demonstrated in Fig.3 in range 100 cm^{-1} ~ 1100 cm^{-1}. The Raman spectra were fitted using the Lorenz and Gaussian functions. The measured and fitted values match well with each other. At *x* value ~ 0.2, 13 vibrational modes are clearly observed in the ceramic. With the increase in *x*, the number of the vibrational modes decreases and it should be attributed to the distortions of MoO_4 tetrahedra. As shown in Fig.3, the A peak located at 141 cm^{-1} corresponds to the translational movement of cation at A-site, and the B peak located at 191 cm^{-1} belongs to the rotation mode between the ion bonds. These spectrum data are in good agreement with that of Porto's report.[21] The D~F peaks located at 388, 425, 466 cm^{-1}, respectively, represent the bending movements of Mo-O, and the I ~ M peaks located at 757, 832, 885, 918, 982 cm^{-1} derive from the stretching movements of Mo-O. When the *x* value rises to 0.95, the intensities of peaks located at 918, 982cm^{-1} gradually weaken and the peaks located at 556, 650cm^{-1} slowly disappear. The peaks located at 321, 885cm^{-1} become narrow and these results may indicate that

the introduction of $(Nd_{1-x}Bi_x)^{3+}$ ions made the MoO_4 tetrahedron become distorted, which possibly affect the position of peaks and lead to the decrease of Raman vibrational modes.

IR patterns of the $[Ca_{0.55}(Nd_{1-x}Bi_x)_{0.3}]MoO_4$ ceramics are shown in Fig.4. It is clearly observed that the measured and fitted IR spectra match well with each other. According to the Eq.(2), there should be 10 IR active vibrational modes in the $[Ca_{0.55}(Nd_{1-x}Bi_x)_{0.3}]MoO_4$ ceramics. However, due to the $(Nd_{1-x}Bi_x)^{3+}$ substitutions, the number of the IR vibrational modes changes and several new vibration modes are observed in this work. As shown in Fig.4, with the increase of *x* value, the Mode-3 peak splits into two new peaks at 0.6 composition, and the Mode-1 peak appears at 0.8 composition. These results are closely related to the translational vibrations of Bi-O (T_{Bi}). Meanwhile, the intensity of Mode-6 observably decreases, the locations of Mode-7 and Mode-8 are shifted by a small amount. These phenomena indicate the increasing disordering in the MoO_4 tetrahedral with the introduction of $(Nd_{1-x}Bi_x)^{3+}$. When the *x* value increases to 0.95, there are two more vibrational modes (1, 4) observed.

The infrared spectra can be analyzed using the Fresnel formula (3) and the Lorentz formula (4) in the typical one-dimensional harmonic oscillator model. Furthermore, these methods are effective to analyze the complex dielectric response of $[Ca_{0.55}(Nd_{1-x}Bi_x)_{0.3}]MoO_4$ ceramics.

$$R(\omega) = \frac{1-\sqrt{\varepsilon'(\omega)}^2}{1+\sqrt{\varepsilon'(\omega)}^2} \tag{3}$$

$$\varepsilon'(\omega) = \varepsilon_\infty + \sum_{j=1}^{n} \frac{\omega_{pj}^2}{\omega_{oj}^2 - \omega^2 - i\gamma_j\omega} \tag{4}$$

where the IR reflectance denoted as R(ω); the dielectric function of R(ω) denoted as ε'(ω); the high-frequency dielectric constant attributed to the electronic polarization denoted as ε_∞; the plasma and transverse frequency denoted as ω_{pj} and ω_{oj}, respectively, γ_j and n represent the damping factor and the phonon mode number, respectively.

In Fig.5, the fitted results of the $[Ca_{0.55}(Nd_{1-x}Bi_x)_{0.3}]MoO_4$ ceramics can be observed. According to the experimental measurement data (sign as red circles in picture), all the measured permittivities are slightly larger than that of the calculated ones. These two results show the same trend with each other. When the *x* value is 0.95, the fitted parameters of $[Ca_{0.55}(Nd_{0.05}Bi_{0.95})_{0.3}]MoO_4$ derived from the IR spectra are listed in Table 1. It is noticed that the calculated permittivity of $[Ca_{0.55}(Nd_{0.05}Bi_{0.95})_{0.3}]MoO_4$ is 19.79, which is a little smaller than the measured one (20.3). Meanwhile, all the measured dielectric losses are similar with the calculated ones. These results indicated that the phonons in infrared regions basically dominated the dielectric polarization of $[Ca_{0.55}(Nd_{1-x}Bi_x)_{0.3}]MoO_4$ ceramics in microwave regions.

The densities of $[Ca_{0.55}(Nd_{1-x}Bi_x)_{0.3}]MoO_4$ ceramics were measured using Archimedes principle and the theoretical densities of these ceramics were calculated with the following formula.[29]

$$\rho_{th} = \frac{nM}{NV} g/cm^3 \quad (5)$$

Where n is the number of per unit cell in the compounds. M and V are molecular weight; the cell volume of the ceramics, respectively, N represents the Avogadro's number (6.022×10^{23} mol^{-1}). Using the measured densities and the theoretical ones, the relative densities of $[Ca_{0.55}(Nd_{1-x}Bi_x)_{0.3}]MoO_4$ ceramics could be calculated with the following equation.

$$\rho_r = \frac{\rho_m}{\rho_{th}} \times 100\% \quad (6)$$

Densities and relative densities of $[Ca_{0.55}(Nd_{1-x}Bi_x)_{0.3}]MoO_4$ ceramics sintered at different temperature are shown in Fig.6 (a ~ f). It can be observed that all the values of density and relative density have the same variation trend. In Fig.6 (a), the maximal density of the $[Ca_{0.55}(Nd_{0.8}Bi_{0.2})_{0.3}]MoO_4$ ceramic is 4.51 g/cm^3, the sintering temperature is 740 ℃. As we know, the bismuth oxide has a low melting point and addition of Bi_2O_3 help reduce the sintering temperature. Therefore, with the x value increasing, the optimal sintering temperature decreases from 740 ℃ to 660 ℃, and the relative density reduces from 95% to 92%. All the samples are well densified and these results are consistent with the SEM results.

Fig.7 (a ~ f) shows the permittivities and Qf values of the $[Ca_{0.55}(Nd_{1-x}Bi_x)_{0.3}]MoO_4$ ceramics as a function of sintering temperature. As presented in Fig.7 (a), the permittivity of $[Ca_{0.55}(Nd_{0.8}Bi_{0.2})_{0.3}]MoO_4$ ceramic increase gradually and then reaches a maximum value at 740 ℃ as the sintering temperature increases. Meanwhile, the Qf value has a quite similar trend vs. sintering temperature. When the x value rises, the sintering temperature of the ceramic with best microwave dielectric properties shifts to the low field, these results are similar to the change of the density and relative density. Then, the optimal sintering temperature of the $[Ca_{0.55}(Nd_{1-x}Bi_x)_{0.3}]MoO_4$ ceramics could be obtained.

The measured microwave dielectric properties of the $[Ca_{0.55}(Nd_{1-x}Bi_x)_{0.3}]MoO_4$ ceramics with optimal sintering temperature are shown in Fig. 8. It is clearly observed that the ε_r value increases from 12.6 to 20.3. According to the Clausius-Mosotti equation, the dielectric constant depends on the polarizability. When the ionic substitution happens, the total ionic polarizability will increase, resulting in an increase of ε_r value. The molecular polarizability of $[Ca_{0.55}(Nd_{1-x}Bi_x)_{0.3}]MoO_4$ ceramics could be estimated by the Shannon's additive rule as follows.[30]

$$\alpha_{[Ca_{0.55}(Nd_{1-x}Bi_x)_{0.3}]MoO_4} = 0.55\alpha_{Ca^{2+}} + 0.3(1-x)\alpha_{Nd^{3+}} + 0.3x\alpha_{Bi^{3+}} + \alpha_{Mo^{6+}} + 4\alpha_{O^{2-}} \quad (7)$$

the polarizability of Bi^{3+} and Nd^{3+} ions are 6.12 Å^3, 5.01 Å^3, respectively. The molecular polarizability increases from 14.63 Å^3 to 14.88 Å^3 as the *x* value increases, indicating that the increasing ε_r value mainly derives from the enhanced cationic polarizability. In this work, the change of relative permittivity is consistent with the Shannon's theory. Generally, the Qf value is inversely proportional to the intrinsic dielectric losses. When the *x* value increases, the expanding unit cell volume and the enhancing disorder lead to the increase of dielectric loss, then the Qf value has a decreasing trend range from 68,380 to 33,860 GHz. The near-zero τ_f value is a significant factor for the microwave ceramic, when *x* value increases, the τ_f value shifts from -52.3 ppm/℃ to -7.1 ppm/℃. The optimal microwave dielectric properties of $[Ca_{0.55}(Nd_{0.05}Bi_{0.95})_{0.3}]MoO_4$ ceramics are obtained at 660 ℃ with a relative permittivity of 20.3, a Qf value of 33,860 GHz (at 7.86 GHz), and a τ_f value of -7.1ppm/℃, this ceramic can be potentially applied in the ULTCC technology. Furthermore, the formulas, the calcinate temperatures and microwave dielectric properties of $[Ca_{0.55}(Nd_{1-x}Bi_x)_{0.3}]MoO_4$ ceramics are listed in Table 2. As shown in Table 2, the ceramics (e.g. x = 0.8, 0.9) sintered at low temperature with excellent microwave dielectric properties can be potentially applied in LTCC technology.

4. CONCLUSION

A series of scheelite-type $[Ca_{0.55}(Nd_{1-x}Bi_x)_{0.3}]MoO_4$ ($0.2 \leq x \leq 0.95$) ceramics are successfully prepared by solid-state reaction method. According to the XRD data, the solid solution was formed and the pure tetragonal phases are clearly observed in the $[Ca_{0.55}(Nd_{1-x}Bi_x)_{0.3}]MoO_4$ ceramics. When the *x* value increases, the sintering temperature of the sample gradually decreases from 740 ℃ to 660 ℃, and the average grain size of the sample also decreases from 3.16 μm to 2.78 μm. These results indicate that the Bi^{3+} ion derived from Bi_2O_3 could effectively lower the sintering temperature and refine grains. Meanwhile, the permittivity is found to increase from 12.6 to 20.3 with increasing *x*, which is due to the enhancement of polarizability derived from Bi^{3+}. The Qf value decreased and gradually remained stable, which is closely related to the rare earth element Nd^{3+}. The Raman spectroscopy showed that the internal modes gradually disappear with increasing *x* value, this phenomenon are due to the distorting MoO_4 tetrahedra, which is also related to the introduction of the $(Nd_{1-x}Bi_x)^{3+}$ ions. The far infrared frequency is close to the microwave frequency, the measured dielectric response from IR spectra can extrapolate to the microwave region. With the fitting data of the IR spectra, the calculated permittivity has the same trend with the measured one, this result indicates that the A-site cations mainly dominate the variation of dielectric response at microwave frequency. The $[Ca_{0.55}(Nd_{0.05}Bi_{0.95})_{0.3}]MoO_4$ ceramic sintered at low temperature (660 ℃) possesses optimal microwave dielectric properties with a relative permittivity of 20.3, a Qf value of 33,860 GHz and a approach zero τ_f value (-7.1 ppm/℃). The $[Ca_{0.55}(Nd_{1-x}Bi_x)_{0.3}]MoO_4$ ceramic system with excellent microwave dielectric properties can be potentially used in LTCC or ULTCC technologies.

ACKNOWLEDGMENTS

This work was supported by the National Key Research and Development Program of China (2017YFB0406301), the State Key Laboratory of Electrical Insulation and Power Equipment (Grant

EIPE19210), the 111 Project of China (B14040) and the Fundamental Research Funds for the Central University. The authors would like to thank the administrators in IR beamline workstation (BL01B) of National Synchrotron Radiation Laboratory (NSRL) for their help in the IR measurement and fitting. The SEM work was done at International Center for Dielectric Research (ICDR), Xi'an Jiaotong University, Xi'an, China and the authors thank Ms. Yan-Zhu Dai for her help in using SEM.

REFERENCE

1. Hill MD, Cruickshank DB. Ceramic materials for 5G wireless communication systems 5G technologies will soon reach the market. Ceramic materials will play an important role in realizing the technology. J Am Ceram Soc B. 2019;98:20-25.

2. Zhou D, Randall CA, Pang LX, Wang H, Guo J, Zhang GQ, et al. Microwave dielectric properties of Li_2WO_4 ceramic with ultra-low sintering temperature. J Am Ceram Soc. 2011;94:348-50.

3. Sebastian MT, Jantunen H. High temperature cofired ceramic (HTCC), low temperature cofired ceramic (LTCC), and ultralow temperature cofired ceramic (ULTCC) materials. J Micro Mater and Appl 2V Set. 2017:355-425.

4. Narang SB, Bahel S. Low loss dielectric ceramics for microwave applications: a review. J Ceram Process Res. 2010;11:316-21.

5. Guo HH, Zhou D, Pang LX, Qi ZM. Microwave dielectric properties of low firing temperature stable scheelite structured (Ca, Bi)(Mo, V)O_4 solid solution ceramics for LTCC applications. J Eur Ceram Soc. 2019;39:2365-73.

6. Guo HH, Zhou D, Liu WF, Pang LX, Wang DW, Su JZ, Qi ZM. Microwave dielectric properties of temperature-stable zircon-type (Bi, Ce)VO_4 solid solution ceramics. J Am Ceram Soc. 2020;103:423-31.

7. Pang LX, Zhou D. Modification of $NdNbO_4$ microwave dielectric ceramic by Bi substitutions. J Am Ceram Soc. 2019;102:2278-82.

8. Chen GH, Di JC, Xu HR, Jiang MH, Yuan CL. Microwave dielectric properties of $Ca_4La_2Ti_{5-x}(Mg_{1/3}Nb_{2/3})_xO_{17}$ ceramics. J Am Ceram Soc. 2012;95:1394-97.

9. Lei W, Zou ZY, Chen ZH, Ullah B, Zeb A, Lan XK, et al. Controllable τ_f value of barium silicate microwave dielectric ceramics with different Ba/Si ratios. J Am Ceram Soc. 2018;101:25-30.

10. Fang L, Li CC, Peng XY, Hu CZ, Wu BL, Zhou HF. $Ba_4LiNb_{3-x}Ta_xO_{12}$(x = 0-3): A series of high-Q microwave dielectrics from the twinned 8H hexagonal perovskites. J Am Ceram Soc. 2010;93:1229-31.

11. Daturi M, Busca G, Borel MM, Leclaire A, Piaggio P. Vibrational and XRD study of the system $CdWO_4$-$CdMoO_4$. J Phys Chem B. 1997;101:4358-69.

12. Kim ES, Jeon CJ, Clem PG. Effects of crystal structure on the microwave dielectric properties of ABO_4 (A = Ni, Mg, Zn and B = Mo, W) ceramics. J Am Ceram Soc. 2012;95:2934-38.

13. Choi GK, Kim JR, Yoon SH, Hong KS. Microwave dielectric properties of scheelite (A= Ca, Sr, Ba) and wolframite (A = Mg, Zn, Mn) $AMoO_4$ compounds. J Eur Ceram Soc. 2007;27:3063-67.

14. Rama Rao SD, Roopas Kiran S, Murthy VRK. Correlation between structural characteristics and microwave dielectric properties of scheelite $Ca_{1-x}Cd_xMoO_4$ solid solution. J Am Ceram Soc. 2012;95:3532-37.
15. Xi HH, Zhou D, Xie HD, He B, Wang QP. Raman spectra, infrared spectra, and microwave dielectric properties of low-temperature firing $[(Li_{0.5}Ln_{0.5})_{1-x}Ca_x]MoO_4$ (Ln = Sm and Nd) solid solution ceramics with scheelite structure. J Am Ceram Soc. 2015;98:587-93.
16. Zhou D, Randall CA, Pang LX, Wang H, Guo J, Zhang GQ, et al. Microwave dielectric properties of $(ABi)_{1/2}MoO_4$ (A = Li, Na, K, Rb, Ag) type ceramics with ultra-low firing temperatures. J Mater Chem and Phys. 2011;129:688-92.
17. Guo J, Randall CA, Zhang GQ, Zhou D, Chen YY, Wang H. Synthesis, structure, and characterization of new low-firing microwave dielectric ceramics: $(Ca_{1-3x}Bi_{2x}\Phi_x)MoO_4$. J Mater Chem C. 2014;2:7364-72.
18. Ha JY, Choi JW, Yoon SJ, Choi DJ, Yoon KH, Kim HJ. Microwave dielectric properties of Bi_2O_3-doped Ca $[(Li_{1/3}Nb_{2/3})_{1-x}Ti_x]O_{3-\delta}$ ceramics. J Eur Ceram Soc. 2003;23:2413-16.
19. Ding JY, Xiao Y, Han PD, Zhang QT. Effects of rare earth oxides on dielectric properties of $Y_2Ti_2O_7$ series ceramics. J rare earth. 2010;28:765-68.
20. Kim ES, Kim SH. Effects of structural characteristics on microwave dielectric properties of $(1-x)CaWO_4$-$xLaNbO_4$ ceramics. J Elect Ceram. 2006;17:471-77.
21. Porto SPS, Scott JF. Raman spectra of $CaWO_4$, $SrWO_4$, $CaMoO_4$, and $SrMoO_4$. J Phys Rev. 1967;157:716.
22. Zheng H, de Györgyfalva GDCC, Quimby R, Bagshaw H, Ubic R, Reaney IM, et al. Raman spectroscopy of B-site order-disorder in $CaTiO_3$-based microwave ceramics. J Eur Ceram Soc. 2003;23:2653-59.
23. Barker Jr AS. Infrared lattice vibrations in calcium tungstate and calcium molybdate. J Phys Rev. 1964;135:A742.
24. Fukuda K, Kitoh R, Awai I. Far-infrared reflection spectra of dielectric ceramics for microwave applications. J Am Ceram Soc. 1994;77:149-54.
25. Kato H, Matsudo N, Kudo A. Photophysical and photocatalytic properties of molybdates and tungstates with a scheelite structure. Chem Lett. 2004;33:1216-17.
26. Shannon RD. Revised effective ionic radii and systematic studies of interatomic distances in halides and chalcogenides. Acta Cryst. 1976;32:751-67.
27. Hao SZ, Zhou D, Pang LX. The spectra analysis and microwave dielectric properties of $[Ca_{0.55}(Sm_{1-x}Bi_x)_{0.3}]MoO_4$ ceramics. J Am Ceram Soc. 2019;102:3103-09.
28. Hanuza J, Maczka M, Macalik L, Van der Maas, J. Polarized raman spectra of $NaBi(MoO_4)_2$ crystal and order-disorder effect in solid scheelites. J Moler Struc. 1994;325:119-24.
29. Liao QW, Li LX, Ren X, Ding X. New low-loss microwave dielectric material $ZnTiNbTaO_8$. J Am Ceram Soc. 2011;94:3237-40.
30. Shannon RD. Dielectric polarizabilities of ions in oxides and fluorides. J Appl Phys. 1993;73:348-66.

Table.1 Values of parameters derived from the fitting of the IR spectra of $[Ca_{0.55}(Nd_{0.05}Bi_{0.95})_{0.3}]MoO_4$

Mode	ω_{oj}	ω_{pj}	γ_j	$\Delta\varepsilon_j$
1	79.94	298.07	55.55	18.2
2	139.59	161.79	39.25	1.7
3	172.8	137.17	32.89	0.708
4	264.95	144.05	41.27	0.681
5	308.36	158.37	65.56	0.302
6	413.13	234.2	71.27	0.306
7	684.13	378.06	91.94	0.355
8	794.55	548.92	60.63	0.477
9	838.12	299.34	33.53	0.128
10	911.01	123.33	21.02	0.018
$\varepsilon_\infty = 2.11$			$\varepsilon_0 = 19.79$	

Table.2 Microwave dielectric properties of the $[Ca_{0.55}(Nd_{1-x}Bi_x)_{0.3}]MoO_4$ ceramics at different sintering temperature as a function of *x* value (mol%).

Compound	S.T(℃)	ε_r	Qf(GHz)	τ_f(ppm/℃)
$[Ca_{0.55}(Nd_{0.8}Bi_{0.2})_{0.3}]MoO_4$	740℃/2h	12.6	68,380	-52.3
$[Ca_{0.55}(Nd_{0.6}Bi_{0.4})_{0.3}]MoO_4$	720℃/2h	14.4	51,530	-45.2
$[Ca_{0.55}(Nd_{0.4}Bi_{0.6})_{0.3}]MoO_4$	700℃/2h	16.8	44,080	-37.5
$[Ca_{0.55}(Nd_{0.2}Bi_{0.8})_{0.3}]MoO_4$	680℃/2h	18.8	35,750	-19.7
$[Ca_{0.55}(Nd_{0.1}Bi_{0.9})_{0.3}]MoO_4$	680℃/2h	19.7	34,540	-11.3
$[Ca_{0.55}(Nd_{0.05}Bi_{0.95})_{0.3}]MoO_4$	660℃/2h	20.3	33,860	-7.1

Figure Captions

Figure 1. (a) The XRD patterns of the $[Ca_{0.55}(Nd_{1-x}Bi_x)_{0.3}]MoO_4$ ceramics at room temperature and the crystal structure of the $[Ca_{0.55}(Nd_{1-x}Bi_x)_{0.3}]MoO_4$ (x = 0.2 ~ 0.95) ceramics (Inset) (b) Lattice parameters of the $[Ca_{0.55}(Nd_{1-x}Bi_x)_{0.3}]MoO_4$ ceramics

Figure 2. (a) The SEM images of $[Ca_{0.55}(Nd_{0.8}Bi_{0.2})_{0.3}]MoO_4$ ceramic sintered at 740°C and the statistic of particle distribution (inset) (b) The SEM images of $[Ca_{0.55}(Nd_{0.05}Bi_{0.95})_{0.3}]MoO_4$ ceramic sintered at 660 ℃ and the statistic of particle distribution (inset)

Figure 3. The observed and calculated Raman spectroscopy of the $[Ca_{0.55}(Nd_{1-x}Bi_x)_{0.3}]MoO_4$ (x = 0.2 ~ 0.95) ceramics

Figure 4. The fitted (black line) and measured (red circles) IR spectra of the $[Ca_{0.55}(Nd_{1-x}Bi_x)_{0.3}]MoO_4$ (x = 0.2 ~ 0.95) ceramics

Figure 5. (a) The real dielectric response, (b) the imaginary dielectric response of the $[Ca_{0.55}(Nd_{1-x}Bi_x)_{0.3}]MoO_4$ (x = 0.2 ~ 0.95) ceramics, the measured data marked as red circles, the fitted data marked as Solid lines

Figure 6. The density and relative density of $[Ca_{0.55}(Nd_{1-x}Bi_x)_{0.3}]MoO_4$ ceramics sintered at different temperature (a) x = 0.2, (b) x = 0.4, (c) x = 0.6, (d) x = 0.8, (e) x = 0.9, (f) x = 0.95.

Figure 7. The permittivities and Qf values of $[Ca_{0.55}(Nd_{1-x}Bi_x)_{0.3}]MoO_4$ ceramics sintered at different temperature (a) x = 0.2, (b) x = 0.4, (c) x = 0.6, (d) x = 0.8, (e) x = 0.9, (f) x = 0.95.

Figure 8. Permittivity, Qf values and τ_f of the $[Ca_{0.55}(Nd_{1-x}Bi_x)_{0.3}]MoO_4$ (x = 0.2 ~ 0.95) ceramics with different sintering temperature

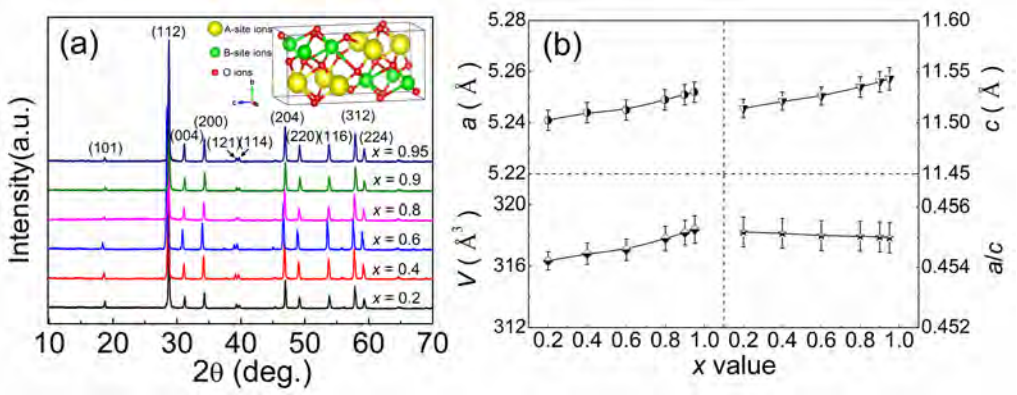

jace_17378_f1.tif

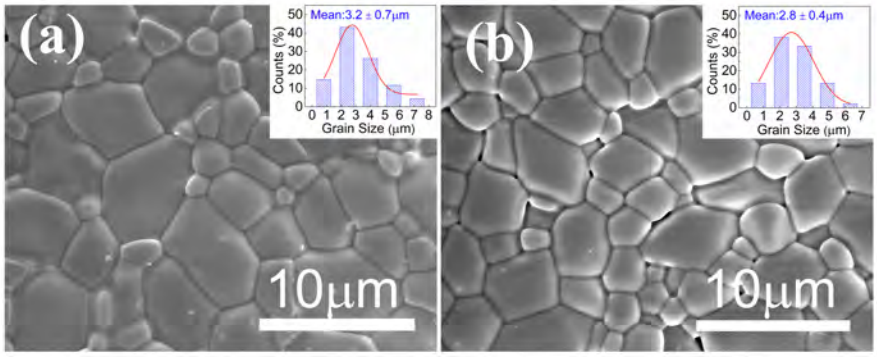

jace_17378_f2.tif

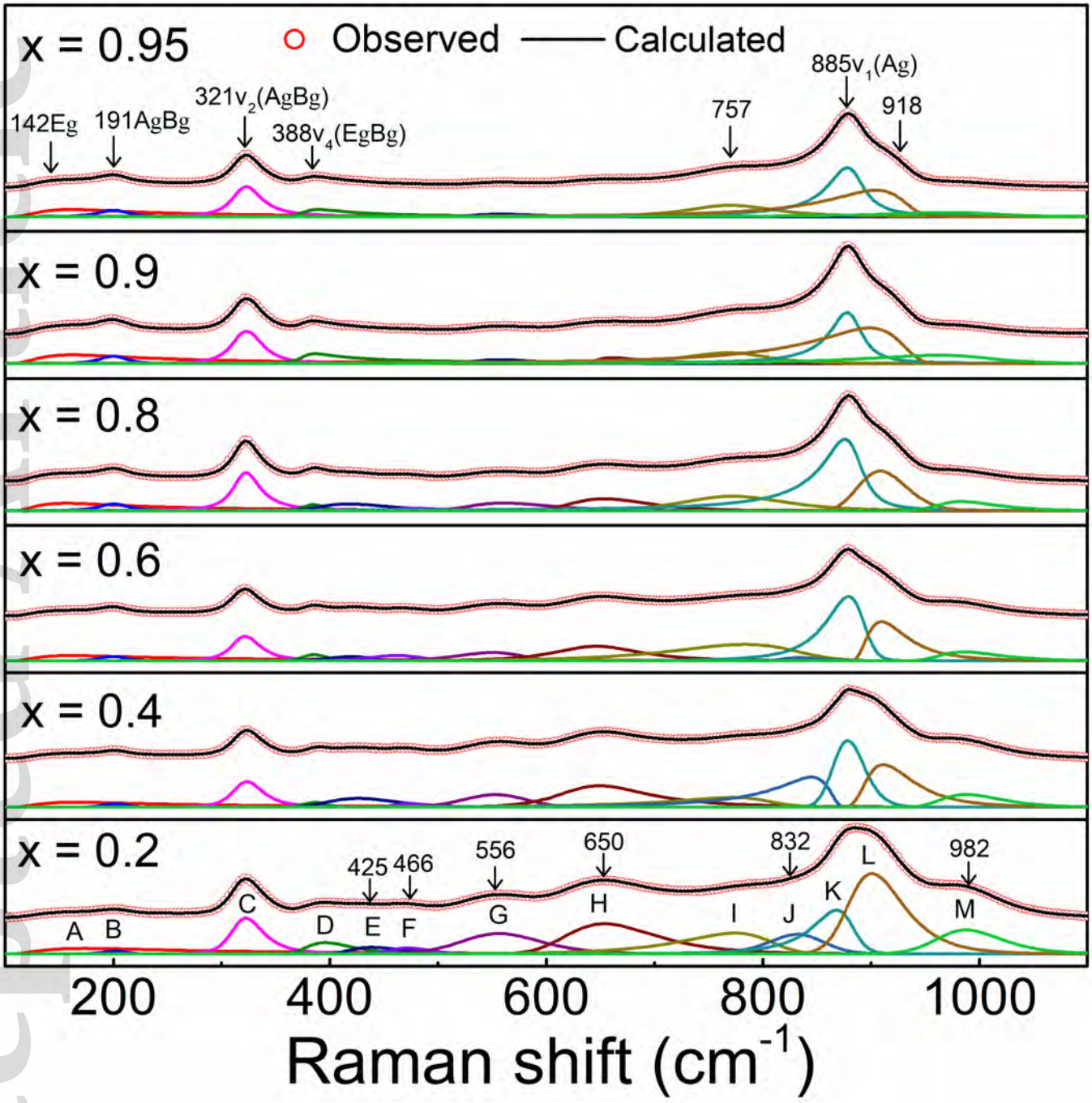

jace_17378_f3.tif

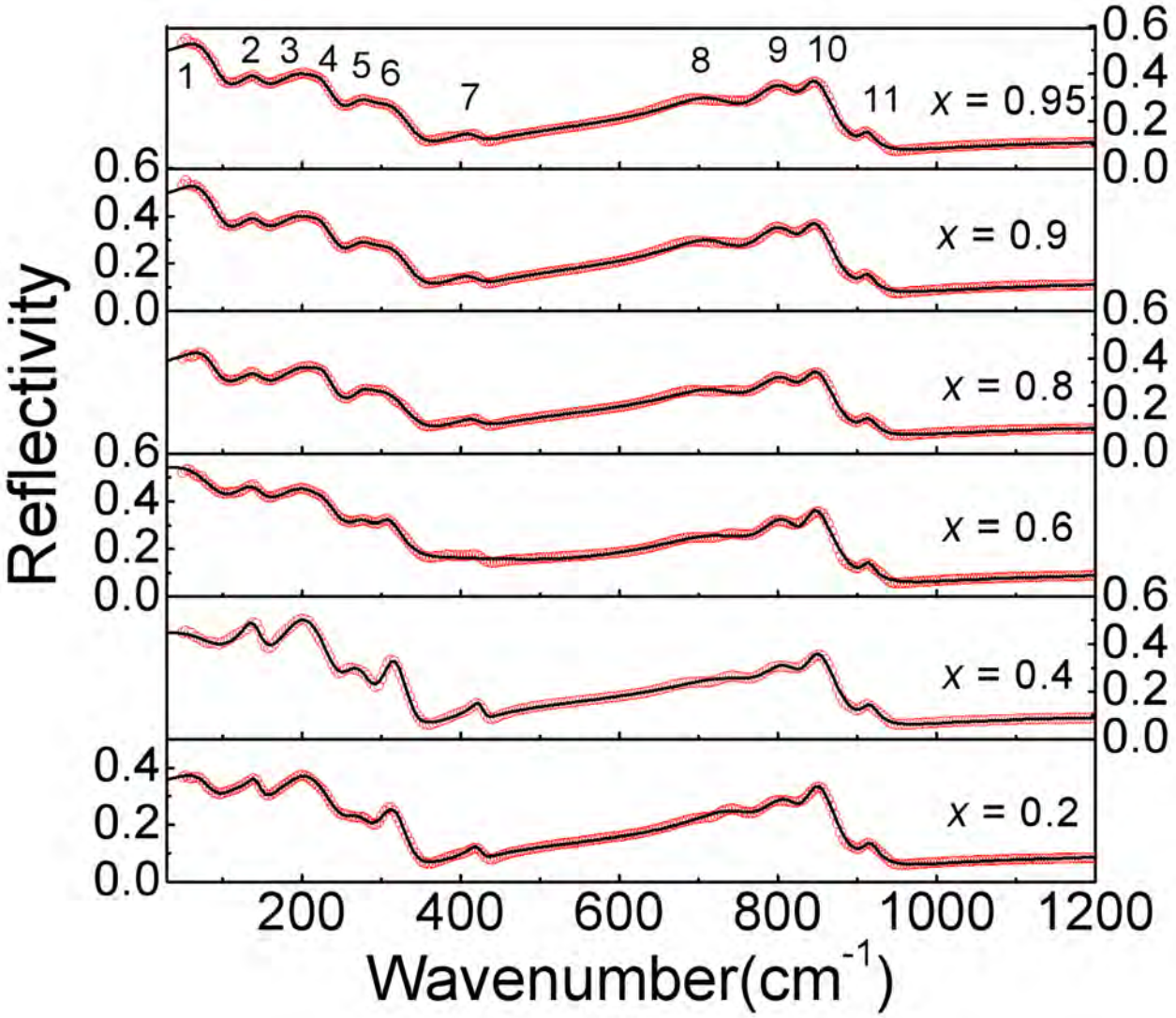

jace_17378_f4.tif

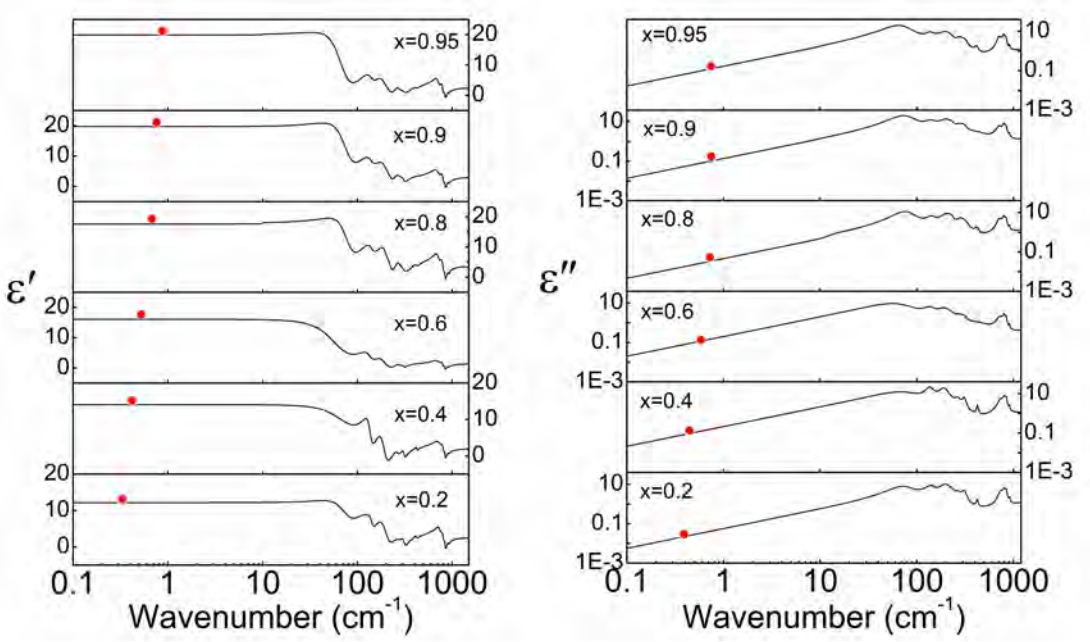

jace_17378_f5.tif

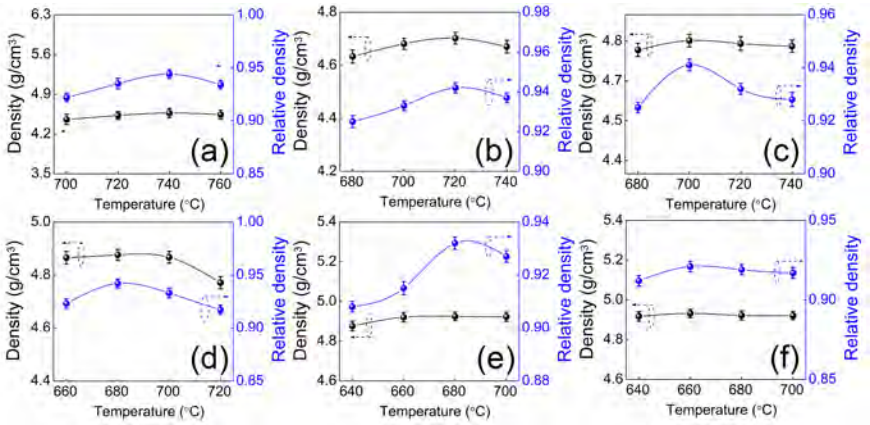

jace_17378_f6.tif

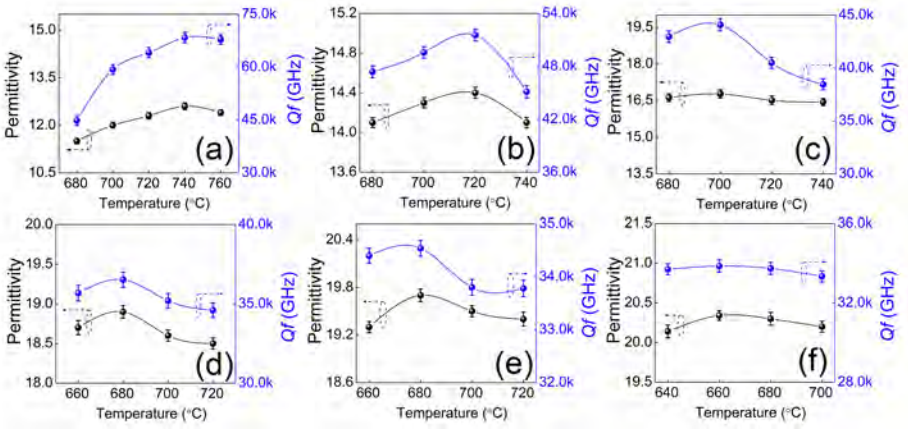

jace_17378_f7.tif

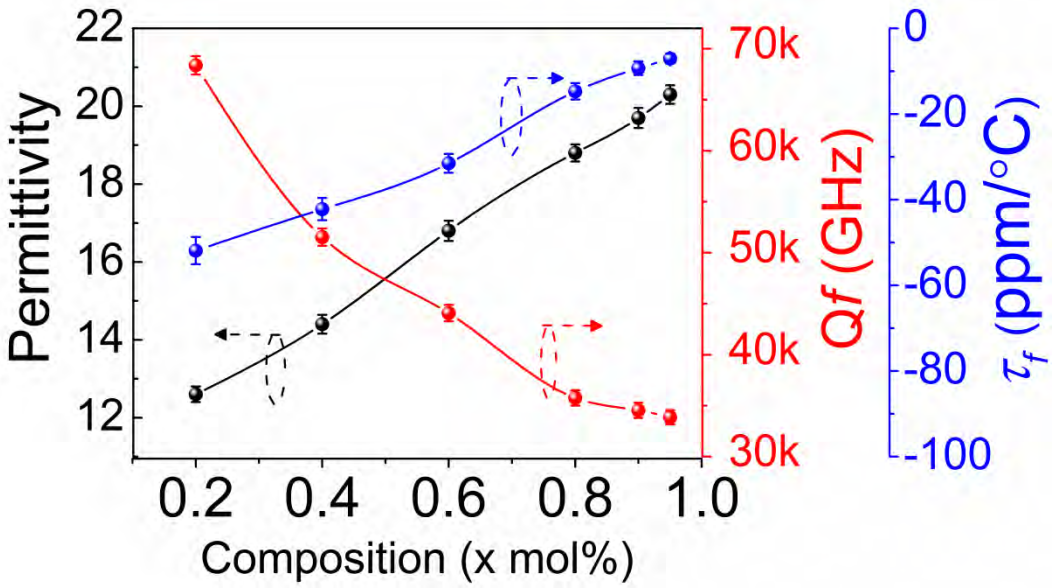

jace_17378_f8.tif